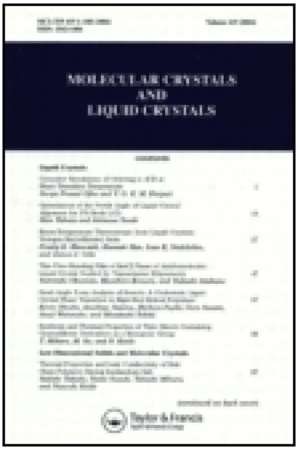

Molecular Crystals and Liquid Crystals
Publication details, including instructions for authors and subscription information:
http://www.tandfonline.com/loi/gmcl20

POLARIZATION HOLOGRAPHIC GRATING BASED ON AZO-DYE-DOPE POLYMER-BALL-TYPE POLYMER-DISPERSED LIQUID CRYSTALS

Andy Ying-Guey Fuh [a] , Chia-Rong Lee [a] & Ting-Shan Mo [a]

[a] Department of Physics, National Cheng Kung University, Tainan, Taiwan 701, Republic of China

Version of record first published: 07 Jan 2010

Mol. Cryst. Liq. Cryst., Vol. 413, pp. 579/[2715]–589/[2725], 2004

ISSN: 1542-1406 print/1563-5287 online
DOI: 10.1080/15421400490439374

POLARIZATION HOLOGRAPHIC GRATING BASED ON AZO-DYE-DOPE POLYMER-BALL-TYPE POLYMER-DISPERSED LIQUID CRYSTALS

Andy Ying-Guey Fuh, Chia-Rong Lee, and Ting-Shan Mo*
Department of Physics, National Cheng Kung University, Tainan, Taiwan 701, Republic of China

A polarization grating (PG) written in an azo-dye-doped film of polymer-ball-type polymer dispersed liquid crystals (PBT-PDLCs) was investigated. The writing beams were two mutually orthogonal (s- and p-polarized) polarized beams. The PG resulted from the LC molecular reorientation due to their interaction with the dye molecules adsorbed on the surface of the polymer balls. Polarization properties of the diffracted beams and the grating pattern were studied under a polarizing optical microscope with a crossed analyzer. The results indicate that the PG diffracts the linearly polarized incident light into beams with different polarizations. Accordingly, the grating can be employed as an un-polarized or polarized beam splitter depending on the polarization of the incident light. The simulation based on the Jones matrix method is developed and the results correspond well with the experimental results.

Keywords: adsorption; Jones matrix; PDLC; polarization grating

INTRODUCTION

Polymer dispersed liquid crystals have recently received increasing interest due to their significant potential for use in displays and light modulators. PDLCs exist the so-called LC-droplet-type [1] and polymer-ball-type [2] (PBT) PDLC films. The former contains micro-sized LC droplets in a polymer matrix, and the latter involves polymer balls in the LC matrix. In addition to scattering light and appearing opaque in the off-state, they can be switched electrically into a transparent-state. These two types differ mainly in the intrinsic memory (hysteresis) effect in the transmission

The authors would like to thank the National Science Council (NSC) of the Republic of China (Taiwan) for financially supporting this research under Contract No. NSC 90-2112-M-006-019.
*Corresponding author. E-mail: andyfuh@mail.ncku.edu.tw

versus applied voltage curve. The memory is highly pronounced only in the PBT-PDLC films. It originates from the interaction at the boundary of polymer and LCs and can be erased if the sample is heated to the isotropic phase, and then cooled down back to room temperature [2].

Holographic grating recordings in photo-polymerizable polymer/LCs composite films is particularly interesting since such gratings can be formed in a single-step process rapidly. Furthermore, the grating is electrically and/or optically switchable [3–5]. Most holographic gratings are intensity gratings, and are recorded without polarization modulation. However, the polarization, rather than the intensity, of polarization holographic gratings (PGs) is modulated. Only a few polarization-sensitive materials have so far been extensively investigated, including photorefractive crystals [6], guest-host systems [7–10], azopolymers [11,12], and PDLCs [13].

Cipparrone *et al.* [13] demonstrated a polarization holographic grating based on the polymer/LCs composites recently. The inferred mechanism is molecular photo-alignment during the formation of PDLCs in photo-polymerization phase separation. In this paper, we report an alternative method of recording a PG in azo-dye-doped PBT-PDLCs. Our previous work showed that the formation of such a PG is attributable to the anisotropic adsorption of dyes on the surface of polymer balls, inducing the reorientation of LCs [14]. Polarization analyses show that the PG diffracts incident linearly polarized light into beams with various polarizations. The Jones matrix method [9,15–17], is employed to develop a model which effectively explains the experimental results.

EXPERIMENTAL

The liquid crystal, monomer, crosslinking agent, and diazo dye used in the experiment were E7 (Merck), di-pentaerythritol pentaacrylate (DPPA; Polysciences), 1-vinyl-2-pyrrolidinone (NVP; Aldrich), and G206 (Nippon Kankoh-Shikiso Kenkyusho), respectively [14]. The mixing ratio of the above components was 70 wt.% of E7, 25 wt.% of DPPA, 5 wt.% of NVP, and 0.5 wt.% of G206. The absorption spectrum of G206 was given in Ref. 5. The homogeneously mixed compounds were sandwiched between two indium-tin-oxide (ITO) coated glass slides separated by a 38-μm-thick plastic spacer to form a sample. The sample was polymerized over around 30 minutes using a strong UV light at an intensity of $\sim 0.2\,\mathrm{W/cm^2}$ to form a translucent PBT-PDLC film [14].

Figure 1(a) shows the experimental setup for writing a polarization holographic grating in this study. The two writing beams, $\mathbf{E}_1$ and $\mathbf{E}_2$, of an Ar^+ laser ($\lambda_w = 514.5\,\mathrm{nm}$) are s- and p-polarized, respectively, and intersect at an angle $\theta \sim 0.9°$. They were unfocused, and each had a power

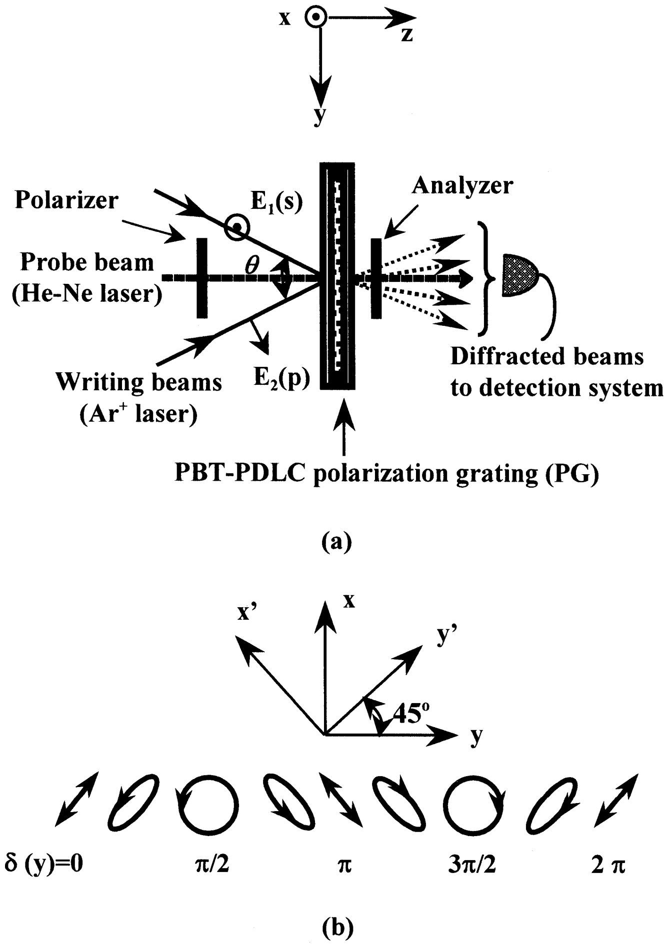

FIGURE 1 (a) Schematic diagram of the experimental setup; (b) configuration of the spatially modulated polarization set up by *s*- and *p*-polarized interfering fields.

of ~150 mW with a beam diameter of ~3.8 mm. A polarization-modulated interference pattern with linear, elliptical, and circular polarizations, was created in the intersecting region, where the sample was placed, as shown in Figure 1(b), since the beams were coherent with mutually perpendicular polarization. The resultant optical field can be written as follows (for small θ) [10].

$$\mathbf{E} \cong [\mathrm{E}_1 \exp(i\delta/2)\mathrm{i} + \mathrm{E}_2 \cos(\theta/2)\exp(-\mathrm{i}\delta/2)\mathrm{j}]\exp\{\mathrm{i}[(2\pi/\lambda_\mathrm{w})\mathrm{z}\cos(\theta/2) - \omega \mathrm{t}]\}, \quad (1)$$

where λ_w is the wavelength of the writing beams in the vacuum, and $\delta = (4\pi/\lambda_w)\,y\,\sin(\theta/2)$ is the phase shift between $\mathbf{E}_1$ and $\mathbf{E}_2$ at $z = 0$. After the PG was formed, the writing beams were switched off and an unpolarized He-Ne probe laser ($\lambda_0 = 632.8\,\text{nm}$) was normally (along z-axis) incident onto the excited region of the sample through a polarizer. An analyzer was placed behind the PG, and then we measured the intensities and the polarization states of the diffracted beams with respect to various polarization of the incident probe beam.

RESULTS AND DISCUSSION

In our recent work, we examined the features of the intensity grating (IG) using two writing beams with the same polarization (s- or p-polarization) in the composite films considered here. The details were presented in Ref. 14. Briefly, the experimental results indicated that the grating had a memory of the polarization of the writing beams. We concluded that the mechanism by which IG is formed in an azo-dye-doped PBT-PDLC film, is the reorientation of the LCs due to their interaction with the anisotropic adsorption of the dye molecules on the surface of the polymer balls. The adsorbed dyes were oriented loosely in the direction perpendicular to both the polarization and propagation directions of the linearly polarized writing beams. The adsorbed dyes then induced the LC molecules to reorient to the same direction as the dye molecules. In this paper, we further studied the PG grating based on similar composite film.

The diffraction efficiencies of the PG written using the setup depicted in Figure 1, probed by a linearly polarized He-Ne laser beam, were measured. The writing time was $\sim$60 seconds. We show the results in Figure 2. The direction of the stripes in the PG was parallel to the x-axis, and $\alpha(\beta)$ was the angle between the transmission axis of the polarizer (analyzer) and the x-axis. Figures 2(a)–2(d) clearly show that the beams diffracted from the formed PGs exhibit various polarization states if the polarization direction of the probe beam varies with respect to the direction of the stripes. Because the third-order (±3) diffracted beams were much weaker than the beams of the other orders ($0, \pm1, \pm2$), they were neglected. When probed by an s-polarized beam, for which $\alpha = 0^\circ$ (Fig. 2(a)), the grating yields even-order diffracted beams with the same polarization as the probe beam, and odd-order beams with a polarization perpendicular to that of the probe beam. Similar results were obtained for the p-polarized probe beam, for which $\alpha = 90^\circ$ (Fig. 2(b)). When the probe beam was polarized at $\alpha = 45^\circ$ and -45° (Fig. 2(c) and 2(d), respectively), the intensities of all the diffracted beams peaked at $\beta = 45^\circ$ and -45°, and vanished at $\beta = -45^\circ$ and 45°. Figure 3 presents the images of PGs under a polarizing

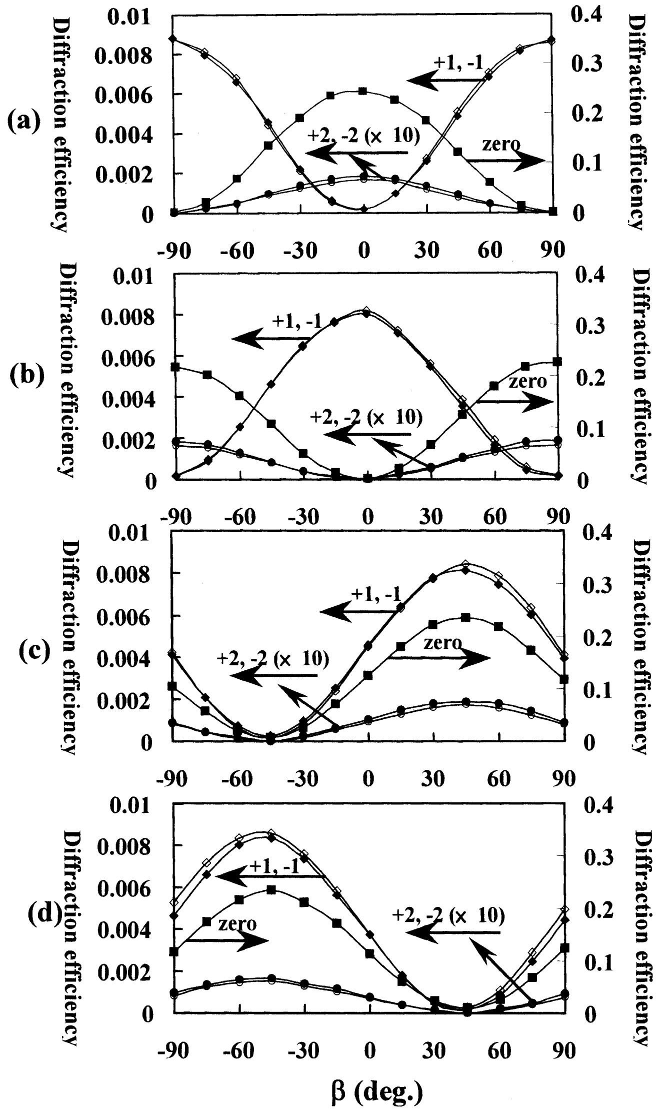

FIGURE 2 Measured diffraction efficiencies of the probe beam with various polarizations as a function of angle, β. (a) $\alpha = 0°$, (b) $\alpha = 90°$, (c) $\alpha = 45°$, and (d) $\alpha = -45°$. α (β) is the angle between the transmission axis of the polarizer (analyzer) and the direction of the stripes (x-axis; refer to Fig. 1). The magnitude of the second order diffracted beam intensity is magnified by ten times.

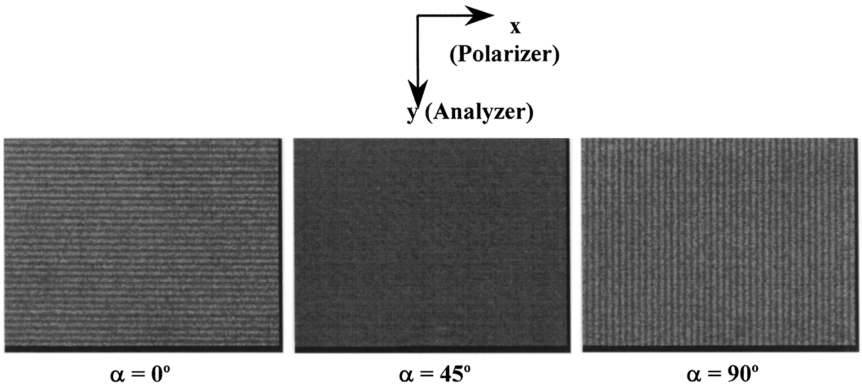

FIGURE 3 Grating patterns observed under a polarizing optical microscope with a crossed analyzer, following the rotation of the stripes of the PG an angle α with the polarizer axis; (a) $\alpha = 0°$, (b) $\alpha = 45°$, and (d) $\alpha = 90°$. The labeled angles are the angles between the direction of the stripes and the polarizer. The grating spacing is 16 μm.

optical microscope with a crossed analyzer. It shows that the grating images (spacing $\sim$16 μm) appear and disappear, if the stripes make angles 0° or 90° and 45°, respectively, with the transmission axis (x-axis) of the polarizer. As mentioned in the first paragraph of this section, we have demonstrated that the azo dyes, after being photo-excited, were adsorbed on the polymer wall with their long axes oriented in the direction perpendicular to both the polarization and the propagation directions of the linearly polarized writing beams [14]. The adsorbed dyes, in turn, reoriented the orientation of the LCs. However, no anisotropic adsorption of dyes occurred if the writing beam was circularly polarized. Accordingly, the observed grating images, shown in Figure 3, can be clearly understood by considering the spatially varying polarization pattern set up by the interference of s- and p-polarized writing beams (Fig. 1(b)) and the inference that LC alignment is due to the adsorbed dyes. Placing the sample between two crossed polarizers makes the grating image to disappear (Fig. 3(b)) when the stripes of the grating make an angle of 45° with the transmission axis of the polarizer since the probe beam is then polarized along the principle axes of the LCs in the sample. However, the image of the grating whose stripes make an angle 0° or 90° appears as shown in Figure 3(a) or 3(c).

As mentioned above, the PBT-PDLC considered here is optically anisotropic only for a linearly polarized writing beam. Such an optical anisotropy is due to light-scattering, but not light absorption. Hence, the birefringence yields a phase grating in the amplitude grating background. The Jones anisotropic matrices due to the phase and amplitude recordings in x′, y′, z′ systems as shown in Figure 1(b) are [9]

$$[\mathbf{T}_\mathrm{P}(\mathrm{y})]_{\mathrm{x}'-\mathrm{y}'} = \exp(\mathrm{i}\phi_0)\begin{bmatrix} \exp(\mathrm{i}\Delta\phi\cos\delta) & 0 \\ 0 & \exp(-\mathrm{i}\Delta\phi\cos\delta) \end{bmatrix}, \text{ and} \tag{2}$$

$$[\mathbf{T}_\mathrm{A}(\mathrm{y})]_{\mathrm{x}'-\mathrm{y}'} = \begin{bmatrix} \mathrm{T}_0 + \Delta\mathrm{T}\cos\delta & 0 \\ 0 & \mathrm{T}_0 - \Delta\mathrm{T}\cos\delta \end{bmatrix}, \tag{3}$$

where $\delta = (4\pi/\lambda_\mathrm{w})\mathrm{y}\sin(\theta/2) = \pi\mathrm{y}/\Lambda$ is the phase shift at $\mathrm{z} = 0$ between the interfering beams. λ_w is the wavelength of the writing beams in the vacuum. $\mathrm{T}_\parallel$ and $\mathrm{T}_\perp$ are the sample amplitude transmissions probed by a beam with its polarization parallel and perpendicular to that of the writing beams, respectively; $\mathrm{T}_0 \equiv (\mathrm{T}_\parallel + \mathrm{T}_\perp)/2$, and $\Delta\mathrm{T} \equiv (\mathrm{T}_\parallel - \mathrm{T}_\perp)/2$. ϕ_0 is equal to $2\pi\mathrm{n}_0\mathrm{d}/\lambda_0$ and n_0 is the refractive index of the sample before the holographic recording. $\Delta\phi = 2\pi\Delta\mathrm{n}\mathrm{d}/\lambda_0$ is the phase shift due to the photo-induced birefringence, $\Delta\mathrm{n} \equiv (\mathrm{n}_\parallel - \mathrm{n}_\perp)/2$ on the PBT-PDLCs; $\mathrm{n}_\parallel$ and $\mathrm{n}_\perp$ are effective indices of the sample that is probed by a probe beam with its polarization parallel and perpendicular to that of the writing beams, respectively. d is the film's thickness, and λ_0 is the probe's wavelength in the vacuum.

The combined Jones matrix can be written as,

$$[\mathbf{T}(\mathrm{y})]_{\mathrm{x}'-\mathrm{y}'} = [\mathbf{T}_\mathrm{P}(\mathrm{y})]_{\mathrm{x}'-\mathrm{y}'}[\mathbf{T}_\mathrm{A}(\mathrm{y})]_{\mathrm{x}'-\mathrm{y}'} = [\mathbf{T}_\mathrm{A}(\mathrm{y})]_{\mathrm{x}'-\mathrm{y}'}[\mathbf{T}_\mathrm{P}(\mathrm{y})]_{\mathrm{x}'-\mathrm{y}'}. \tag{4}$$

Transformation into the x–y coordinate system [15] yields,

$$[\mathbf{T}(\mathrm{y})]_{\mathrm{x}-\mathrm{y}} = \mathbf{S}(-45^\circ)[\mathbf{T}(\mathrm{y})]_{\mathrm{x}'-\mathrm{y}'}\mathbf{S}(45^\circ), \tag{5}$$

where $\mathbf{S}$ is the transformation matrix. Since $\Delta\mathrm{n}$ is usually small, that is $\Delta\mathrm{n} << 1$ in the PBT-PDLCs, Eq. (5) can be rewritten as,

$$[\mathbf{T}(\mathrm{y})]_{\mathrm{x}-\mathrm{y}} = \frac{\exp(\mathrm{i}\phi_0)}{2\begin{bmatrix} (\mathrm{a}+\mathrm{b}) & (\mathrm{a}-\mathrm{b}) \\ (\mathrm{a}-\mathrm{b}) & (\mathrm{a}+\mathrm{b}) \end{bmatrix}}, \tag{6}$$

where a and b are the terms $(\mathrm{T}_0 \pm \Delta\mathrm{T}\cos\delta)(1 \pm \mathrm{i}\Delta\phi\cos\delta - \Delta\phi^2\cos^2\delta/2)$ with the signs, " + " and " − ", respectively.

The Jones vector of the probe beam that emerges from the PG, $\mathbf{E}_\mathrm{t}(\mathrm{y})$, is [16]

$$\mathbf{E}_\mathrm{t}(\mathrm{y}) = \mathbf{T}(\mathrm{y})\mathbf{E}_\mathrm{i}, \tag{7}$$

where $\mathbf{E}_\mathrm{i}$ is the Jones vector for the incident probe beam, and may be expressed as,

$$\mathbf{E}_\mathrm{i} = \mathrm{E}_{\mathrm{i}0}\begin{bmatrix} \cos\alpha \\ \sin\alpha \end{bmatrix}. \tag{8}$$

The transmitted optical field can be expressed as a vectorial Fourier expansion form as below, since diffraction via the PG is paraxial [16,17]. (Raman-Nath type; the third-order diffracted beam in the present case makes an angle of $\sim 3.5^\circ$ with respect to the zeroth order (z-axis)).

$$\mathbf{E}_t(y) = \sum_{m=-\infty}^{m=\infty} \mathbf{D}_m \exp(i2\pi m y/\Lambda), \tag{9}$$

where $\Lambda (= 16\,\mu m)$ is the spacing of the grating, and m is an integer. The polarization states of the mth-order diffracted beam is determined by the Fourier components, $\mathbf{D}_m(\alpha)$, of the transmitted field [16].

$$\mathbf{D}_m(\alpha) = (1/\Lambda) \int_0^\Lambda \mathbf{E}_t(y) \exp(-i2\pi m y/\Lambda) dy, \tag{10}$$

where α is the angle made by the probe-beam's polarization with the x-axis (Fig. 1). Substituting Eqs. (6)–(9) into Eq. (10), yields a general expression for the mth-order diffracted beams:

$$\mathbf{D}_m(\alpha) = E_{i0} \exp(i\phi_0) \begin{bmatrix} (a_0\delta_{m,0} + a_2\delta_{m,\pm 2}) \cos\alpha + (a_1\delta_{m,\pm 1} + a_3\delta_{m,\pm 3}) \sin\alpha \\ (a_0\delta_{m,0} + a_2\delta_{m,\pm 2}) \sin\alpha + (a_1\delta_{m,\pm 1} + a_3\delta_{m,\pm 3}) \cos\alpha \end{bmatrix}, \tag{11}$$

where $\delta_{m,n} = 0$ or 1 if $m \neq n$ or $m = n$, respectively. Therefore, the mth components of the diffracted beam are,

$$\begin{aligned} \mathbf{D}_0 &= E_{i0} \exp(i\phi_0) a_0 \begin{bmatrix} \cos\alpha \\ \sin\alpha \end{bmatrix}, \mathbf{D}_{\pm 1} = E_{i0} \exp(i\phi_0) a_1 \begin{bmatrix} \sin\alpha \\ \cos\alpha \end{bmatrix}, \\ \mathbf{D}_{\pm 2} &= E_{i0} \exp(i\phi_0) a_2 \begin{bmatrix} \cos\alpha \\ \sin\alpha \end{bmatrix}, \mathbf{D}_{\pm 3} = E_{i0} \exp(i\phi_0) a_3 \begin{bmatrix} \sin\alpha \\ \cos\alpha \end{bmatrix}, \end{aligned} \tag{12}$$

where a_0, a_1, a_2, and a_3 are $[T_0(1 - \Delta\phi^2/4) + i\Delta T \Delta\phi/2]$, $[\Delta T (1 - 3\Delta\phi^2/8)/2 + iT_0\Delta\phi/2]$, $[-T_0\Delta\phi^2/8 + i\Delta T\Delta\phi/4]$, and $[-\Delta T \Delta\phi^2/16]$, respectively.

The diffracted fields through the analyzer can be specified as

$$\mathbf{D}_m(\alpha, \beta) = \mathbf{A}(\beta)\mathbf{D}_m(\alpha) = \begin{bmatrix} \cos^2\beta & \sin\beta\cos\beta \\ \sin\beta\cos\beta & \sin^2\beta \end{bmatrix} \mathbf{D}_m(\alpha), \tag{13}$$

where $\mathbf{A}$ is a matrix that represents the analyzer whose transmission axis makes an angle β with the x-axis. The diffraction efficiencies through the analyzer are defined as,

$$\eta_m \equiv |\mathbf{D}_m(\alpha, \beta)|^2 / |\mathbf{E}_i|^2. \tag{14}$$

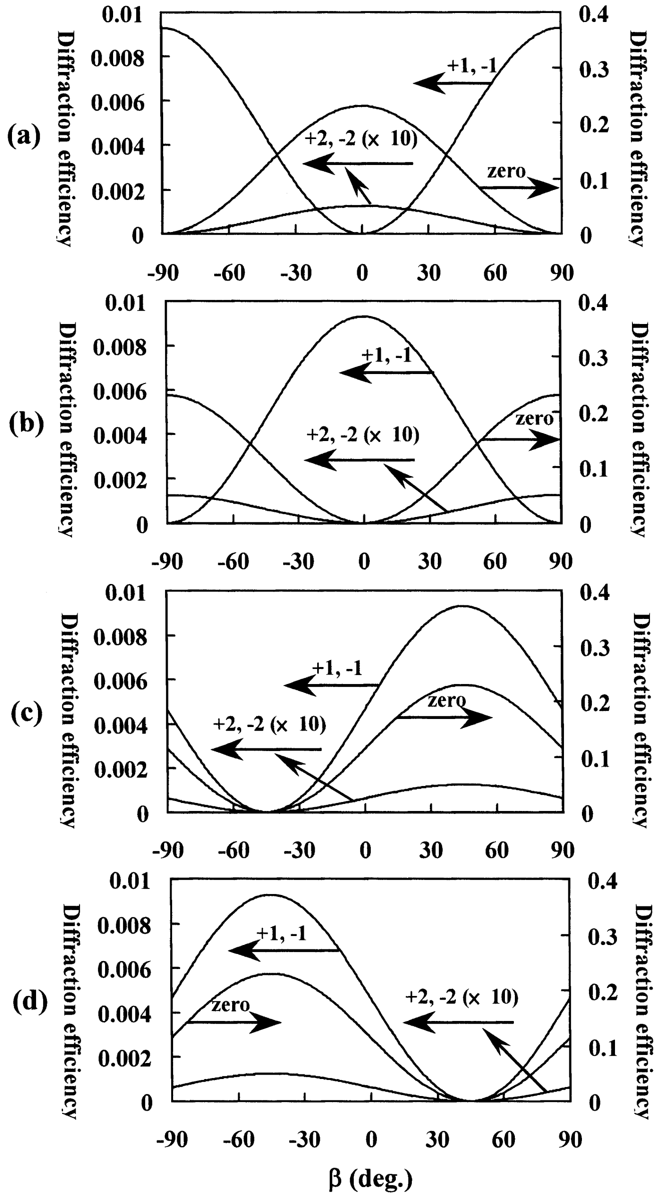

FIGURE 4 Simulated diffraction efficiencies of the sample, under the conditions that yielded the results in Figure 2. The magnitude of the second order diffracted beam intensity is magnified by ten times.

An additional experiment was carried out to estimate the values of $T_{\parallel}$ and $T_{\perp}$. Five PBT-PDLC samples were excited identically by a single s-polarized pump beam for $\sim$60 s and, then, the average amplitude transmission of the probe beam with s- and p-polarization, $T_{\parallel}$ and $T_{\perp}$, were measured to be $\sim$0.62 and 0.36, respectively. Hence, ΔT ($\equiv(T_{\parallel} - T_{\perp})/2$) and $T_0(\equiv(T_{\parallel} + T_{\perp})/2)$ were 0.13 and 0.49, respectively. Based on the measured results in Figure 2, the average value of ${a_0}^2$ is calculated to be $\sim$0.23. Substituting the above values of ΔT, T_0 and ${a_0}^2$ into a_0 $(= T_0(1 - \Delta\phi^2/4) + i\Delta T\Delta\phi/2)$ defined in Eq. (12), we obtain an effective birefringence value (Δn) to be $\sim 8 \times 10^{-4}$. From Eq. (12), the other amplitude of diffraction efficiencies, ${a_1}^2$, and ${a_2}^2$, were, therefore, determined to be 9.3×10^{-3} and 1.25×10^{-4}, respectively. Substituting the above values, $a_{i = 0 \sim 2}$, into Eq. (14) yields the simulated diffraction efficiencies through the analyzer, as shown in Figures 4(a)–(d). These results agree closely with the experimental results shown in Figure 2.

CONCLUSIONS

We used two mutually orthogonal and linearly polarized recording beams (s- and p-polarized) to record a polarization grating in a PBT-PDLC film doped with an azo-dye. The formation of the PG was attributable to the interaction between the LCs and the photo-excited dye molecules adsorbed on the surface of the polymer balls. Polarization analysis show that the polarization of the diffracted beams depends on that of the incident light. Therefore, a PG can be used as a polarized or unpolarized beam splitter, depending on the polarization of incident light. The Jones matrix method was used to explain the polarization characteristics of the beams diffracted from the PG formed on the azo-dye-doped PBT-PDLCs. A six-month old PG sample was tested, and showed no significant aging effect. Thus, the memory time is long. Also, the result obtained recently using similar material indicates that it is possible to write a more efficient PG by increasing the concentration of azo-dye [18].

REFERENCES

[1] Doane, J. W., Vaz, N. A., Wu, B.-G., & Zumer, S. (1986). *Appl. Phys. Lett.*, *48*, 269–272.
[2] Yamaguchi, R. & Sato, S. (1991). *Jpn. J. Appl. Phys.*, *30*, L616–L618.
[3] Sutherland, R. L., Tondiglia, V. P., & Natarajan, L. V. (1994). *Appl. Phys. Lett.*, *64*, 1074–1076.
[4] Fuh, A. Y.-G., Ko, T.-C., Tsai, M.-S., Huang, C.-Y., & Chien, L.-C. (1998). *J. Appl. Phys.*, *83*, 679–683.
[5] Andy Y.-G. Fuh, Tsai, M.-S., Huang L.-J., & Liu, T.-C. (1999). *Appl. Phys. Lett.*, *74*, 2572–2574.

[6] Sturman, B. I., Goul'kov, M. Yu., & Odoulov, S. G. (1996). *J. Opt. Soc. Am. B*, *13*, 577–583.
[7] Khoo, I. C. (1991). *Mol. Cryst. Liq. Cryst.*, *207*, 317–329.
[8] Slussarenko, S., Francescangeli, O., & Simoni, F. (1997). *Appl. Phys. Lett.*, *71*, 3613–3615.
[9] Nikolova & Todorv, T. (1984). *Opt. Acta*, *31*, 579–588.
[10] Anderle, K. & Wendorff, J. H. (1994). *Mol. Cryst. Liq. Cryst.*, *243*, 51–75.
[11] Naydenova, I., Nikolova, L., Todorov, T., Holme, N. C., Ramanujan, P. S., & Hvilsted, S. (1998). *J. Opt. Soc. Am. B*, *15*, 1257–1265.
[12] Lagugne Labarthet, F. & Rochon, P. (1999). *Appl. Phys. Lett.*, *75*, 1377–1379.
[13] Cipparrone, G., Mazzulla, A., & Russo, G. (2001). *Appl. Phys. Lett.*, *78*, 1186–1188.
[14] Fuh, A. Y.-G., Lee, C.-R., Ho, Y.-H., Mo, T.-S., & Liu, P.-M. (2001). *Jpn. J. Appl. Phys.*, *40*, 6868–6871.
[15] Kliger, D. S., Lewis, J. W., & Randall, C. E. (1990). *Polarized Light in Optics and Spectroscopy*, Academic: Boston.
[16] Tervo, J. & Turunen, J. (2000). *Opt. Lett.*, *25*, 785–786.
[17] Turunen, J., Wyrowski, F., & Noponen, E. (1994). *Diffractive and Holographic Optics Technology*, Cindrich, I. & Lee, S. H. (Eds)., Proc SPIE 2152, 34–43.
[18] Fuh, A. Y.-G., Liao, C.-C., Hsu, K.-C., Lu, C.-L., & Tsai, C.-Y. (2001). *Opt. Lett.*, *26*, 1767–1769.